Simultaneous biogas upgrading and centrate treatment in an outdoors pilot scale high rate algal pond

Esther Posadas[1], David Marín[1,3], Saúl Blanco[2], Raquel Lebrero[1], Raúl Muñoz*[1]

[1] Department of Chemical Engineering and Environmental Technology, Valladolid University, Dr. Mergelina, s/n, 47011, Valladolid, Spain.

[2] Department of Biodiversity and Environmental Management, University of León, 24071 León, Spain.

[3] Universidad Pedagógica Nacional Francisco Morazán, Boulevard Centroamérica, Tegucigalpa, Honduras.

* Corresponding author: mutora@iq.uva.es

ABSTRACT

The bioconversion of biogas to biomethane coupled to centrate treatment was evaluated in an outdoors pilot scale high rate algal pond interconnected to an external CO_2-H_2S absorption column (AC) via settled broth recirculation. CO_2-removal efficiencies ranged from 50 to 95% depending on the alkalinity of the cultivation broth and environmental conditions, while a complete H_2S removal was achieved regardless of the operational conditions. A maximum CH_4 concentration of 94% with a limited O_2 and N_2 stripping was recorded in the upgraded biogas at recycling liquid/biogas ratios in the AC of 1 and 2. Process operation at a constant biomass productivity of 15 g m^{-2} d^{-1} and the minimization of effluent generation supported high carbon and nutrient recoveries in the harvested biomass (C = 66±8%, N= 54±18%, P≈100% and S =16±3%). Finally, a low diversity in the structure of the microalgae population was promoted by the environmental and operational conditions imposed.

Keywords: algal-bacterial symbiosis, biogas upgrading, biomethane, microalgae, outdoors conditions, wastewater treatment.

1. Introduction

Biogas from the anaerobic digestion of organic solid waste and wastewater represents a renewable energy source with a significant potential to reduce the current world´s fossil fuel dependence (Hermann et al., 2016). Biogas can be used as a fuel for the on-site generation of domestic heat or steam and electricity in industry, as a substrate in fuel cells or as a substitute of natural gas prior upgrading (Andriani et al., 2014; Muñoz et al., 2015). For instance, the use of this biofuel in the European Union during 2014 supported a production of electricity and heat of 63.4 and 32.2 TWh, respectively (EBA, 2016). Biogas conversion to biomethane is highly recommended due to the high concentration of impurities present in the raw biogas: CO_2 (25-60%), CO (<0.6%), H_2S (0.005-2%), N_2 (0-2%), NH_3 (<1%), H_2O (5-10%), O_2 (0-1%), siloxanes (0-0.02%) and halogenated hydrocarbons (VOC <0.6%) (Ryckebosch et al., 2011). In fact, biogas upgrading is a mandatory step required prior biomethane injection into natural gas grids or use as a vehicle fuel, which must provide concentrations of $CH_4 \geq 95\%$, $CO_2 \leq 2\%$, $O_2 \leq 0.3\%$ and negligible amounts of H_2S according to most international regulations (Muñoz et al., 2015). In this context, the removal of CO_2 from raw biogas would contribute to reduce the transportation costs and to increase the calorific value of biomethane, while the removal of H_2S would limit the corrosion in pipelines, boilers, engines, etc. (Posadas et al., 2015a).

Several physical-chemical and biological technologies are nowadays available at commercial scale to remove CO_2 and H_2S from biogas. Pressure swing adsorption, amine/water/organic scrubbing or membrane separation are typically applied to remove CO_2, while activated carbon filtration, chemical precipitation or anoxic/aerobic biotrickling filtration provide satisfactory levels of H_2S removal (Mann et al., 2016; Toledo-Cervantes et al., 2016; Muñoz et al., 2015). However, these H_2S and CO_2

removal technologies must be sequentially implemented to remove both biogas contaminants, which makes physical-chemical biogas upgrading a costly and complex two-stage process (Muñoz et al., 2015). The few technologies supporting a simultaneous removal of CO_2 and H_2S from low S-strength biogas (i.e. chemical scrubbing) exhibit high environmental impacts and operating costs (Tippayawong and Thanompongchart, 2010). In this context, algal-bacterial photobioreactors have recently emerged as an environmentally friendly and cost-efficient alternative to remove CO_2 and H_2S from raw biogas in a single step process (Bahr et al., 2014; Yan et al., 2016).

Photosynthetic biogas upgrading in algal-bacterial photobioreactors is based on the simultaneous fixation of CO_2 by microalgae and oxidation of H_2S to SO_4^{2-} by sulfur oxidizing bacteria or chemical reactions, the latter supported by the high dissolved oxygen (DO) concentrations present in the cultivation broth (Posadas et al., 2015a; Toledo-Cervantes et al., 2016). The economic and environmental sustainability of this process can be boosted via integration of biogas upgrading with the recovery of nutrients from digestate in the form of a valuable algal-bacterial biomass (Serejo et al., 2015; Posadas et al., 2015a, 2016; Toledo-Cervantes et al., 2016; Yan et al., 2016).

Several investigations aiming at integrating photosynthetic biogas upgrading with digestate treatment have been recently carried out in indoors high rate algal ponds (HRAPs) interconnected to biogas absorption columns (AC) under artificial illumination (Bahr et al. 2014; Alcántara et al., 2015; Posadas et al. 2015a, 2016; Serejo et al. 2015; Meier et al. 2015; Toledo-Cervantes et al. 2016, 2017). Despite the rapid optimization of this technology (Toledo-Cervantes et al., 2016, 2017), the constant temperature (often in the optimum range) and irradiation (often too low compared to solar irradiation) prevailing under laboratory conditions still hinder the complete understanding of a process designed to be ultimately implemented outdoors under solar irradiation. Therefore, the evaluation of the performance of photosynthetic biogas upgrading under outdoors conditions is crucial to understand the influence of the diurnal variations of light irradiance and temperature on the quality of the upgraded biogas. Similarly, process operation to minimize the desorption of O_2 and N_2 from the cultivation broth to the upgraded biogas, and to maximize nutrient recovery from digestates, must be optimized to the particular conditions prevailing during outdoors operation.

Despite the remarkable environmental advantages of using digestates as a nutrient source during biogas upgrading, their high nutrients content results in high biomass concentrations in the HRAPs (7-50 g L^{-1}) and the need to operate the process at low digestates flowrates. This severely decreases the photosynthetic efficiency of the system as a result of mutual shading and entails a net consumption of water to compensate evaporation losses (Posadas et al., 2016). In this context, all studies carried out to date set the make-up water input to maintain similar effluent and influent flowrates in order to guarantee a constant biomass output, which resulted in the generation of effluents with residual nutrient concentrations (Toledo-Cervantes et al., 2016; Posadas et al., 2016). On this basis, there is an urgent need to develop novel photobioreactor designs and operational strategies to minimize effluent generation while maintaining high microalgae productivities using digestates as a nutrient source.

This work aimed at evaluating the potential of a novel pilot scale HRAP interconnected to an AC via recirculation of the settled cultivation broth under outdoors conditions during the simultaneous upgrading of biogas and treatment of centrate. Process performance was evaluated under pseudo-steady state conditions at different alkalinity levels and make-up water supply regimes from June to October. Under each operational stage, process performance was also assessed during one diurnal cycle of temperature and irradiance. A novel strategy decoupling biomass productivity from the effluent flowrate via control of the biomass wastage from the settler was applied to maximize the recovery of carbon and nutrients from biogas and centrate in the form of harvested biomass. Finally, the influence of the recycling liquid/biogas (L/G) ratio on the efficiency of biogas upgrading was also evaluated during a 24 h diurnal cycle.

2. Materials and methods

2.1 Biogas and centrate

A synthetic biogas mixture, composed of CO_2 (29.5%), H_2S (0.5%) and CH_4 (70%), was used as a model biogas (Abello Linde; Spain). Centrate was obtained from the centrifuges dehydrating the anaerobically digested sludge of Valladolid wastewater treatment plant and stored at 4 ºC prior to use. Centrate composition along the experimental period was subjected to the typical variations of real wastewaters: total organic carbon (TOC) = 70±8 mg L^{-1}, inorganic carbon (IC) = 522±40 mg L^{-1}, total nitrogen (TN) = 580±102 mg L^{-1}, $N\text{-}NH_4^+$ = 553±67 mg L^{-}, $P\text{-}PO_4^{3-}$ = 34±7 mg L^{-1} and SO_4^{2-} = 9±9 mg L^{-1}.

2.2 Experimental set-up

The pilot plant was located outdoors at the Department of Chemical Engineering and Environmental Technology of Valladolid University (41.39º N, 4.44º W). The experimental set-up consisted of a 180 L HRAP with an illuminated surface of 1.20 m^2 (length = 170 cm; width = 82 cm; depth =15 cm) and two water channels divided by a central wall and baffles in each side of the curvature. The HRAP was interconnected to an external 2.5 L bubble absorption column (internal diameter = 4.4 cm; height = 165 cm) provided with a metallic gas diffuser (2 μm pore size) located at the bottom of the column. The HRAP and AC were interconnected via external liquid recirculation of the supernatant of the algal-bacterial cultivation broth from an 8 L settler located at the outlet of the HRAP (Fig. 1). The internal recirculation velocity of the cultivation broth in the HRAP was ≈ 20 cm s^{-1}, which was provided by the continuous rotation of a 6-blade paddlewheel.

<Figure 1>

2.3 Operational conditions and sampling procedures

Process operation was carried out from June 29th to October the 4th 2016. Based on a previous study conducted by Norvill et al. (2017) in a similar HRAP treating urban wastewater at 4 days of hydraulic retention time (HRT) in the same location, a constant biomass productivity of 15 g m^{-2} d^{-1} was set throughout the 92 days of operation. The required C, N and P input to maintain this biomass productivity was 9.7 g C d^{-1}, 1.9 g N d^{-1} and 0.2 g P d^{-1}, assuming a C, N and P biomass content of 45, 9 and 1%, respectively (Posadas et al., 2015b). This required a centrate flow rate of 3.2 L d^{-1} (considering an IC and N-NH_4^+ stripping of 20%, and the absence of P removal by precipitation; Posadas et al. (2013)) and a biogas flow rate of 74.9 L d^{-1} (assuming an average CO_2 removal efficiency in the AC of 80% based on Posadas et al. (2015a)). The recycling liquid/biogas (L/G) ratio in the AC was fixed at 0.5 according to Toledo-Cervantes et al. (2016). The liquid and biogas residence time in the AC under these operational conditions were 96 and 48 min, respectively. The settled biomass in the settler was continuously recirculated to the HRAP at a flow rate of 7.2 L d^{-1}. This, together with the external recycling, resulted in a HRT in the settler of 4.4 h. This process configuration has been shown to increase the settleability of the algal-bacterial biomass, while avoiding biomass degradation in the settler (Valigore et al., 2012; Park et al., 2011, 2013). Biomass harvesting was performed by daily removing the required settled biomass volume according to its total suspended solids (TSS) concentration in order to maintain the above mentioned biomass productivity.

The HRAP was initially filled with tap water (IC = 550 mg L^{-1}) and inoculated to an initial concentration of 210 mg TSS L^{-1} with *Chlorella* sp. from a HRAP treating centrate at the Department of Chemical Engineering and Environmental Technology of Valladolid University (Spain). The system was inoculated on June 29th, and after 5 d of inoculum acclimation batchwise, three different operational conditions were tested (corresponding to stages I, II and III) to optimize the simultaneous outdoors biogas upgrading and centrate treatment from a technical and environmental view point (Table 1).

<Table 1>

Stage I (reference state) was conducted at a centrate IC concentration of 522 ± 40 mg C L^{-1}. During stages II and III, the IC concentration of the centrate was increased up to 2024±124 mg C L^{-1} by addition of $NaHCO_3$ and Na_2CO_3, which increased the pH of the centrate from 8.38±0.33 in stage I to 9.94±0.09 and 10.06±0.13 in stages II and III, respectively (Table 1). Tap water was fed to the HRAP in stages I and II to compensate evaporation losses and maintain an effluent flowrate of 0.6±0.4 and 0.8±0.4 L d^{-1}, respectively, thus minimizing the loss of carbon, nutrients and fresh water. The effluent from the system was returned to the HRAP in stage III to minimize the supply of $NaHCO_3$ and Na_2CO_3, with a subsequent decrease in the supply of make-up water. Each operational stage was maintained for approximately one month, where temperature, solar irradiation and number of sun hours remained approximately constant (Table 1). The results obtained for the liquid phase throughout the three operational stages were provided as average values along with their corresponding standard deviation from measurements recorded for four consecutive days during each steady state.

The ambient and cultivation broth temperatures, influent and effluent flowrates, DO and pH in the cultivation broth, and the photosynthetic active irradiation (PAR) were daily monitored. Gas samples of 100 µL of the raw and upgraded biogas were drawn twice a week to monitor the concentrations of CO_2, H_2S, CH_4, O_2 and N_2. The inlet and outlet biogas flowrates in the AC were also measured to accurately determine both CO_2 and H_2S removals, and CH_4 losses by absorption. Liquid samples of 100 mL from the centrate and the treated effluent after settling were withdrawn twice a week to monitor the pH, TSS concentration, and concentrations of dissolved TOC, IC, TN, $N\text{-}NH_4^+$, $N\text{-}NO_2^-$, $N\text{-}NO_3^-$, $P\text{-}PO_4^{3-}$ and SO_4^{2-} following sample filtration through 0.20 µm nylon filters. Likewise, liquid samples of 25 mL were drawn from the cultivation broth and from the bottom of the settler twice a week to monitor the algal-bacterial TSS concentration. The algal-bacterial biomass harvested from the settler under steady state was washed three times with distilled water and dried for 24 hours at 105 ºC to determine its elemental composition (C, N, P and S). Process monitoring and biomass harvesting were always conducted at 9:00 a.m. along the entire experimental period.

At the end of each operational stage, the outdoors temperature and PAR, along with the temperature, DO concentration and pH in the HRAP, settler and AC were measured every 30 minutes during one entire diurnal cycle from one hour prior to dawn to one hour after sunset. The composition and flowrate of the upgraded biogas were recorded every hour, and the concentrations of TOC, IC and TN in the HRAP, settler and AC were analyzed every 2 hours.

2.4 Influence of the L / G ratio on the quality of the upgraded biogas

L/G ratios ranging from 0.5 to 5 were tested at the end of stage III (4th - 7th October) to optimize the quality of the upgraded biogas. A biogas flowrate of 74.9 L d^{-1} was maintained while the liquid flowrates were set at 37.5, 74.9, 149.8 and 374.5 L d^{-1} (providing L/ G ratios of 0.5, 1, 2 and 5, respectively). Each L/G ratio was maintained for 12 h during one-day diurnal cycle. The ambient temperature and PAR, along with the temperature, DO and pH in the HRAP, settler and AC, and the composition and flowrate of the upgraded biogas, were measured every two hours from one hour prior to dawn to one hour after sunset.

2.5 Analytical procedures

The monthly average ambient temperatures, PARs and number of sun hours were provided by the official AEMET meteorological station located at the University of Valladolid. CO_2, H_2S, CH_4, O_2 and N_2 gas concentrations were determined using a Varian CP-3800 GC-TCD (Palo Alto, USA) according to Posadas et al. (2015a). Temperature and DO concentration were determined using an OXI 330i oximeter (WTW, Germany). An Eutech Cyberscan pH 510 (Eutech instruments, The Netherlands) was used for pH determination. The PAR was measured with a LI-250A light meter (LI-COR Biosciences, Germany). The concentrations of dissolved TOC, IC and TN were measured using a Shimadzu TOC-VCSH analyzer (Japan) coupled with a TNM-1 chemiluminescence module. $N\text{-}NH_4^+$ concentration was determined with an ammonium specific electrode Orion Dual Star (Thermo Scientific, The Netherlands). The concentrations of $N\text{-}NO_3^-$, $N\text{-}NO_2^-$, $P\text{-}PO_4^{3-}$ and SO_4^{2-} were quantified by HPLC-IC according to Posadas et al. (2013). All analyses were carried out according to Standard Methods (APHA, 2005).

The determination of the C, N and S content of the algal-bacterial biomass was conducted in a LECO CHNS-932 analyzer, while phosphorus content was determined spectrophotometrically after acid digestion in a microwave according to Standard Methods (APHA, 2005). The identification, quantification and biometry measurements of the microalgae assemblage under steady state were performed by microscopic examination (OLYMPUS IX70, USA) of biomass samples (fixed with lugol acid at 5% and stored at 4 ºC prior to analysis) according to Sournia (1978).

3. Results and discussion

3.1. Environmental parameters

The average ambient temperature, PAR and number of sun hours slightly decreased from stage I (July) to stage III (September), which is inherent to outdoors environmental conditions in European latitudes (Table 1). Despite these variations, the environmental conditions were comparable throughout the three experimental stages and therefore the imposed operational conditions can be considered the main parameters influencing process performance.

The DO concentration, temperature and pH in the cultivation broth of the HRAP during a diurnal cycle at the end of each operational stage were directly correlated with the ambient temperature and light irradiance (Fig. A.1-A.4). Hence, the DO concentration in the HRAP during steady state in stages I, II and III fluctuated from 1.4 to 15.6, 1.3 to 16.7 and 0.9 to 13.2 mg O_2 L^{-1}, respectively (Fig. A.2). Microalgae activity was not inhibited at such low-moderate DO concentrations, since pernicious effects on photosynthesis are typically encountered above 25 mg O_2 L^{-1} (Molina et al., 2001). The average temperature and pH in the cultivation broth of the HRAP under steady state during stages I, II and III were 25±6, 25±6 and 19±5ºC, and 8.9±0.4, 10.0±0.0 and 9.9±0.0, respectively (Fig. A.3 and A.4). The higher pH recorded in stages II and III was attributed to the higher pH of the centrate fed to the system compared with that used during stage I. Moreover, the lower buffer capacity of the cultivation broth in this first operational stage (Table 1; Fig. A.5) resulted in significant variations of the pH along the day (from 8.3 to 9.4), which confirmed the key role of alkalinity for pH control in algal-bacterial photobioreactors (Posadas et al., 2013). The lower pH values recorded in the AC compared to those in the HRAP, regardless of the operational stage, were due to the acidification of the recycling broth caused by the absorption of CO_2 and

H_2S (Posadas et al., 2016) (Fig. A.4). Despite these sharp daily variations in temperature, DO and pH, all parameters remained in the acceptable range to support microbial activity (Posadas, 2016).

Finally, the evaporation rates during stages I, II and III accounted for 7±2 L, 9±1 and 3±2 L m^{-2} d^{-1}, respectively (Fig. A.6). The highest evaporation rate here recorded was ~1.5 times higher than the maximum predicted for an arid area by Guieysse et al. (2013). These high values were attributed to the high temperatures and turbulence in the HRAP as a result of the typical oversizing of the motor of the paddlewheel in lab scale-pilot systems (Posadas et al., 2015c; Guieysse et al., 2013). In this context, the scale-up of this experimental set-up will likely entail lower evaporation rates.

3.2 Biogas upgrading

The composition of the biomethane obtained during stage I significantly varied depending on the environmental conditions compared to stages II and III, where the concentration of all biogas components remained approximately constant (Fig. 2). CH_4 concentrations in the upgraded biogas during stage I ranged from 72 to 93 %, while the removal efficiencies (REs) of CO_2 and H_2S ranged from 50 to 75 % and from 91 to 100%, respectively. Average CH_4 concentrations of 90±2 % and 91±1 % were recorded in the upgraded biogas during stages II and III, respectively, along with CO_2-REs of 86±4% and a complete H_2S removal regardless of the operational conditions (Fig. 2a). These results also showed that the absence of effluent in stage III did not influence the quality of the upgraded biogas. O_2 and N_2 concentrations in the biomethane during the three operational stages ranged from 0.1 to 2.0% and from 0.6 to 5.0%, respectively, depending on the pH of the cultivation broth and on the alkalinity (Fig. 2c). These values were only slightly higher than those reported by Toledo-Cervantes et al. (2016) during the indoors operation of a similar process at a L/G ratio of 1, which validated the results obtained under laboratory conditions. CH_4 absorption in the AC was negligible, with average losses of 2.2±1.2% (on a mass basis) along the three operational stages. The biomethane composition obtained was both compliant with international regulations for injection into natural gas grids in Europe (i.e. Belgium and The Netherlands) and Latin-America (i.e. Chile), and suitable for use as autogas (Muñoz et al., 2015).

<Figure 2>

The main fluctuations in the composition of the upgraded biogas were recorded during stage I, which were attributed to the diurnal variations in irradiation and temperature. In this context, the concentrations of CH_4, CO_2, H_2S, O_2 and N_2 in the upgraded biogas ranged from 70.5 to 86.8%, 8.8 to 24.7%, 0 to 0.1%, 0.7 to 1.1% and 2.6 to 4.2%, respectively, during the diurnal cycle evaluated in stage I (Fig. 3). The increase in the alkalinity of the cultivation broth during stages II and III (from 267±56 mg IC L^{-1} in stage I to 2174±253 and 2660±48 mg IC L^{-1} during stages II and III, respectively) reduced the variability in the composition of the upgraded biogas. In this sense, CH_4, CO_2, O_2 and N_2 concentrations in stage II ranged from 87 to 92%, 5 to 9%, 0 to 1% and 1 to 3%, respectively, while in stage III these concentrations varied from 85 to 93%, 4 to 12%, 0 to 2% and 1 to 3%, respectively (Fig. 3). H_2S was completely removed in both stages.

The highest CO_2-REs, which entailed also the highest CH_4 concentrations in the upgraded biogas, were recorded at the lowest ambient temperature regardless of the operational stage as a result of the higher solubility of CO_2 (Sander, 1999). A 60% decrease in CO_2 solubility is expected when temperature increases from 10 to 40°C (Sander, 1999). However, the high CO_2 concentration gradient supported by the high alkalinity of the cultivation broth in stages II and III compensated the decrease in CO_2

solubility mediated by the 30 °C temperature increase (Fig. A.3). The correlation between the temperature of the cultivation broth in the settler and the CO_2 concentration in the upgraded biogas was only significant during stage I. This result suggested that CO_2 absorption in a low alkalinity media is controlled by the influence of the temperature on the aqueous solubility of CO_2 (according to the Henry´s Law constant) (Sander, 1999). However, the influence of the temperature on the concentration of O_2 or N_2 in the upgraded biogas was negligible likely due to their limited aqueous solubility (Fig. A.7). These results confirmed the high influence of the ionic strength of the recycling cultivation broth on the quality of the upgraded biogas (Bahr et al. 2014). The higher CO_2-REs recorded in stages II and III compared to stage I were likely mediated by the pH increase in the cultivation broth, which significantly enhanced the CO_2 concentration gradient (Bahr et al. 2014; Toledo-Cervantes et al. 2016). The CO_2-REs here reported were always higher than those recorded by Bahr et al. (2014) during simultaneous biogas upgrading and centrate treatment (≈40%), and similar to those obtained by Serejo et al. (2015), who reported an average CO_2-RE of ≈80% at a L/G ratio of 10 during the upgrading of biogas combined with the treatment of diluted anaerobically digested vinasse.

<Figure 3>

The high aqueous solubility of H_2S (three times higher than that of CO_2) resulted in high H_2S-REs, comparable to those recorded in previous studies carried out under laboratory conditions (Bahr et al., 2014; Posadas et al., 2015a; Serejo et al., 2015; Toledo-Cervantes et al., 2016; Lebrero et al., 2016). A complete H_2S removal was observed in stages II and III due to the higher pH of the cultivation broth (Fig. 2b), which was in agreement with the results obtained by Bahr et al. (2014). H_2S oxidation ratios (defined as the ratio between the mass of S-SO_4^{2-} in the HRAP cultivation broth and the mass of H_2S absorbed in the AC) of 36±13, 47±9 and 47±7 % were recorded during stages I, II and III, respectively. In this sense, an incomplete H_2S oxidation to SO_4^{2-} was also observed by Toledo-Cervantes et al. (2016) and Lebrero et al. (2016) likely due to the low O_2 concentration in the absorption column. Despite the fact that the highest DO concentrations were achieved during stage I, the lowest H_2S oxidation ratio recorded in this period was associated to the effect of the temperature on the solubility of the H_2S in a low ionic strength medium and therefore, to the limited H_2S mass transfer efficiency from the biogas to the liquid phase.

3.3 Influence of the L/G ratio on the quality of the upgraded biogas

The similar PAR and outdoor temperatures recorded during the five consecutive days of this study allowed an unbiased comparison of the influence of the L/G ratio on biomethane composition (Fig. A. 8). In fact, similar DO concentrations and temperature profiles were recorded in the HRAP regardless of the tested L/G ratio (Fig. A. 9), although the pH of the cultivation broth in the HRAP and AC varied depending on the L/G ratio tested (Figs. A.9-A.11). Thus, the daily average pH of the cultivation broth in the AC was 8.8±0.1, 9.4±0.1, 9.6±0.1 and 9.8±0.8 at L/G ratios of 0.5, 1, 2 and 5, respectively (Fig. A.10). This pH increase at higher L/G ratios was attributed to the lower CO_2 transferred per volume of recycling cultivation both, which prevented the acidification of the broth in the AC.

<Figure 4>

L/G ratios > 1 supported a significant decrease in CO_2 concentration in the upgraded biogas, which ranged from 1.8 to 3.7% and corresponded to CO_2-REs ≈ 95% (Fig. 4b). The increase in pH in the cultivation broth of the AC at increasing L/G ratios supported higher CO_2 concentrations gradient between the biogas and liquid phase, which enhanced CO_2-REs (Posadas et al., 2016). In our particular study, the maximum CO_2

mass transfer capacity was achieved at a L/G ratio of 1. In this context, Serejo et al. (2015) recorded a maximum CO_2 mass transfer (CO_2-RE of 95±2%) at a L/G ratio of 15, pH of 8 and IC concentrations ≈80 mg L^{-1}, respectively. On the other hand, Toledo-Cervantes et al. (2016) recorded a CO_2-RE of 98.8±0.2% regardless of the tested L/G (0.5-60) at a pH of 10 and IC concentration ≈4000 mg L^{-1}. These studies confirmed the key role of the alkalinity of the recycling cultivation broth on the biogas upgrading efficiency compared to other operational parameters.

H_2S was completely removed regardless of the tested ratio likely due to its high aqueous solubility (Bahr et al., 2014; Serejo et al., 2015). The O_2 and N_2 concentration in the upgraded biogas only increased significantly at a L/G ratio of 5 (up to 5.5% and 12.8%, respectively) (Fig. 4c, 4d). Indeed, the increase in the L/G ratio mediated a higher desorption of O_2 and N_2 from the recycling, which negatively impacted the final concentration of CH_4 in the upgraded biogas. In this context, the maximum CH_4 concentration (94%) was obtained at L/G ratios of 1 and 2 (Fig. 4a).

3.4 Wastewater treatment performance

The wastewater treatment efficiency of the HRAP was evaluated under pseudo-steady state at the three operational stages evaluated (Fig. 5; Figs. A12-A13).

<Figure 5>

The TOC effluent concentrations, which ranged from14 to 85 mg L^{-1}, were similar to the influent TOC concentrations due to the low biodegradability of the centrate, the concentration effect caused by the high water evaporation rates in the HRAP and the low or negligible effluent flowrates (Posadas et al., 2013; 2015c) (Fig. 5a). Despite the low DO concentrations recorded in the cultivation broth (<2 mg O_2 L^{-1}) in the early morning could have partially limited organic matter oxidation (Metcalf and Eddy, 2003), the removals of TOC estimated by mass balance calculations ranged from 59±7% (stage III) to 74±7% (stage I) (Table 2) (Fig. A.3).

<Table 2>

The TIC-REs in stage I were higher than those recorded in stages II and III as a result of the higher inorganic carbon feeding and C-CO_2 REs in the AC during these latter stages (Table 2). Therefore, only 65±6 and 66±8% of the total carbon removed in stages II and III was recovered in the harvested biomass, while a 97±1% carbon recovery was observed during stage I (Table 3). Despite the higher pH values should have promoted lower IC removals by stripping based on the limited CO_2 aqueous equilibrium concentration, the lower IC loading during stage I resulted in a lower fraction of C removed by stripping (Table 3) (Posadas et al., 2013) (Fig. 5b).

Similar TN-REs of 86±4, 87±4 and 80±4% were recorded during stages I, II and III, respectively, while a complete N-NH_4^+ removal occurred during the entire experimental period (Table 2; Fig. 5c, 5d). Nitrification was not inhibited by the high pH values prevailing during stages II and III or the low DO concentrations (<1 mg O_2 L^{-1}) present in the first hours in the morning (Fig. A.3). N-NO_2^- concentrations were low compared to N-NO_3^- despite temperatures higher than 28ºC were always recorded close to midday, which are known to promote the partial oxidation of N-NH_4^+ (Fig. 5e; Figs. A.2-A.3) (Metcalf and Eddy, 2003). The oxidation ratios (referred to [N-NO_3^-+ N-NO_2^-] mass outputs compared to TN mass input, Posadas et al. (2015a)) were 11±2, 13±4 and 19±8% during stages I, II and III, respectively. The high nitrification activity, together with the high evaporation rates, induced an increase in N-NO_3^- concentration in the cultivation broth up to 148 mg L^{-1} in stage I, 198 mg L^{-1} in stage II and 293 mg L^{-1} in stage III, this latter increase mediated by the absence of effluent from the HRAP (Fig. 5f). The nitrogen recovered in the harvested biomass accounted for 65±3, 54±18 and

76±19% of the total nitrogen removed during stages I, II and III, respectively (Table 3). These values were considerably higher than those recorded by Posadas et al. (2015a) (45±7%) and Toledo-Cervantes et al. (2017) (19±13% and 36±18%) in a similar indoors experimental set-up during the simultaneous treatment of biogas and digestates as a result of the lower microalgae productivities in those studies.

<Table 3>

High P-PO_4^{3-} REs of 92±2, 84±5 and 85±5% were recorded during stages I, II and III, respectively (Table 2). The higher P-RE in stage I was likely mediated by the higher P content of the harvested biomass (Table 3). In this regard, P-PO_4^{3-} concentration in the cultivation broth increased up to 6 mg L^{-1} in stage I, 15 mg L^{-1} in stage II and 17 mg L^{-1} in stage III. These increasing P-PO_4^{3-} concentration were also supported by the evaporation rate and the low or negligible effluent flowrates (Fig. 5g). A P mass balance revealed than approximately 100% of the P removed was recovered in the harvested biomass, despite high pH values are known to promote PO_4^{3-} precipitation (Cai et al., 2013) (Table 3).

Finally, H_2S oxidation supported an increase in SO_4^{2-} concentration in the cultivation broth of the HRAP from 60 to 495 mg L^{-1} through the 92 operational days, also triggered by the high evaporation rates and low effluent flowrates (Fig. 5h). The fraction of H_2S not fully oxidized to sulphate would have remained as S-intermediates in the liquid phase (S°, thiosulfate or sulfite) (Toledo-Cervantes et al., 2016). This was confirmed by the observation of S° accumulation on the walls and diffuser of the AC during stage I (Photograph 1, appendix), while a S mass balance revealed that only 26±5, 17±3 and 16±3% of the S removed was recovered in the harvested biomass during stages I, II and III, respectively (Table 3). Further analyses to determine the actual sulfur compounds present in the cultivation broth are required.

3. 5 Concentration and composition of the algal-bacterial biomass

The steady state biomass concentrations in the HRAP during stages I, II and III averaged 660±17, 1078±84 and 665±79 mg TSS L^{-1} (Fig. A. 14). The operational strategy here evaluated based on the control of biomass productivity via regulation of the settled biomass wastage rate successfully maintained the concentration of algal-bacterial biomass below light limiting values. At this point it should be stressed that the theoretical biomass concentration generated based on the centrate composition would be ≈2000 mg TSS L^{-1} (with P as the limiting nutrient). The good settling characteristics of the algal-bacterial (supporting TSS-REs in the settler of 80±9%) were likely promoted by the short HRT in the settler and the continuous recirculation of the settled biomass, which boosted the enrichment of rapidly settling algal-bacterial flocs (Valligore et al., 2011; Park et al., 2011).

The elemental composition of the harvested biomass remained within the typical range reported in literature, regardless of the operational stage (Posadas et al., 2016; Bi et al., 2013). C, N and P content in the biomass decreased from stage I to stage II and slightly increased in stage III (Table 3). The different C/N/P (g/g/g) ratios present in the cultivation broth of the HRAP (100/39/2, 100/6/1 and 100/12/1 during stages I, II and III, respectively) could have influenced this final biomass composition, despite the C/N ratio in the harvested biomass remained always at the optimum value of 6 regardless of the operational conditions (Serejo et al., 2015). The main differences were recorded in the S content, which decreased from 0.4% in stage I to 0.2% in stages II and III (Table 3). The higher S content in the biomass was recorded concomitantly with the occurrence of S precipitation (Photograph 1, appendix), and was attributed to the likely S absorption into the biomass.

The inoculated *Chlorella* sp. was gradually replaced by *Chloroidium saccharophilums* (*Chlorella saccharophila)* during stage I. *Chloroidium saccharophilum* was the dominant microalga species during stage I (94%) and stage III (100 %), while *Pseudanabaena* sp. accounted for 6% and 54% of the total number of microalgae cells in stages I and II, respectively (Fig. 6). *Pseudanabaena* sp. has been consistently found in a similar indoors experimental set-up during the simultaneous upgrading of biogas and digested vinasse treatment (Posadas et al. 2015a; Serejo et al. 2015). The lower microalgae diversity recorded outdoors compared to that observed under laboratory conditions in a similar experimental set-up was likely due to i) the recirculation of the settled biomass and ii) the high alkalinity in the cultivation broth in stages II and III (Serejo et al., 2015; Posadas et al., 2015a; Toledo-Cervantes et al., 2016, 2017; Park et al., 2011).

<Figure 6>

4. Conclusions

This work constitutes the first proof-of-concept study of photosynthetic biogas upgrading coupled with centrate treatment at pilot scale under outdoors conditions. The feasibility of a zero-effluent process operation was also demonstrated. Temperature played a key role on the efficiency of biogas upgrading at low-to-medium alkalinities, while high alkalinities enhanced process robustness against daily temperature variations. Process operation at L/G ratios of 1-2 provided a biomethane complying with most international regulations. A consistent centrate treatment was achieved regardless of the operational conditions, while the decoupling of biomass productivity from the HRT allowed high recoveries of C, N and P.

ACKNOWLEGMENTS

This research was supported by MINECO and the European Union through the FEDER program (CTM2015-70442-R and Red Novedar), the Regional Government of Castilla y León (Project VA024U14 and UIC 71) and INIA (RTA2013-00056-C03-02). The authors wish to thanks Julia Bilbao and Argimiro de Miguel from the Atmosphere and Energy Laboratory at Valladolid University for kindly providing the temperature, radiation data and number of sun hours. Valladolid University is also acknowledged for funding the research contract of Esther Posadas.

REFERENCES

(1) Alcántara C., García-Encina P., Muñoz R., 2015. Evaluation of simultaneous biogas upgrading and treatment of centrates in a HRAP through C, N and P mass balances. Water Sci. Technol. 72, 150-157.

(2) Andriani D., Wresta A., Atmaja T., Saepudin A., 2014. A review on optimization production and upgrading biogas through CO_2 removal using various techniques. Appl. Biochem. Biotechnol. 172, 1909–1928.

(3) APHA; AWWA; WEF. Standard Methods for the Examination of Water and Wastewater; 21st ed.; Washington, 2005.

(4) Bahr M., Díaz I., Domínguez A., González Sánchez A., Muñoz R., 2014. Microalgal-biotechnology as a platform for integral biogas upgrading and nutrient removal from anaerobic effluents. Environ. Sci. Technol. 48, 573-581.

(5) Bi Z., He B. B., 2013. Characterization of microalgae for the purpose of biofuel production, Transactions of the ASABE, Vol. 56 (4), 1529-1539.

(6) Cai T., Park S.Y., Li Y., 2013. Nutrient recovery from wastewater streams by microalgae: Status and prospects. Renew. Sust. Energ. Rev. 19, 360-369.

(7) European Biogas Association (EBA): ATBEST International Conference 7-8 September (2016), Linköping by Arthur Wellinger.

(8) Guieysse B., Béchet Q., Shilton A., 2013. Variability and uncertainty in water demand and water footprint assessments of fresh algae cultivation based on case studies from five climatic regions. Bioresour. Technol. 128, 317–323.

(9) Herrmann C., Kalita N., Wall D., Xia A., Murphy J. D., 2016. Optimised biogas production from microalgae through co-digestion with carbon-rich co-substrates. Bioresour. Technol. 214, 328-337.

(10) Lebrero R., Toledo-Cervantes, Muñoz R., Del Nery V., Foresti E., 2016. Biogas upgrading from vinasse digesters: a comparison between ananoxic biotrickling filter and an algal-bacterial photobioreactor. J. Chem. Technol. Biotechnol. 91 (9), 2488-2495.

(11) Mann G., Schlegel M., Kanswohl N., Schumann R., 2016. Experimental system for the prevention of O_2– and air contamination during biogas upgrading with phototrophic microalgae. Appl Agric Forestry Res. DOI: 10.3220/LBF1471268642000.

(12) Meier L., Pérez R., Azócar L., Rivas M., Jeison D. 2015. Photosynthetic CO_2 uptake by microalgae: an attractive tool for biogas upgrading. Biomass and bioenergy, 73, 102-109.

(13) Metcalf, Eddy, 2003. Wastewater Engineering and Reuse, 4th ed., New York, Mc. GrawHill.

(14) Molina E., Fernández J. M., Acién F. G., Chisti Y., 2001. Tubular photobioreactors design for algal cultures. J. Biotechnol. 92, 113-131.

(15) Muñoz R., Meier L., Díaz I, Jeison D., 2015. A review on the state-of-the-art of physical/chemical and biological technologies for biogas upgrading. Rev. Environ. Sci. Biotechnol. 14, 727–759.

(16) Norvill Z., Toledo-Cervantes A., Blanco S., Shilton A., Guieysse B., Muñoz R., 2017. Photodegradation and sorption govern tetracycline removal during wastewater treatment in algal ponds. Bioresource Technology (submitted for publication).

(17) Park J.B.K., Craggs R.J., Shilton A.N., 2013. Enhancing biomass energy yield from pilot-scale high rate algal ponds with recycling. Water Res. 47 (13), 4422-4432.

(18) Park J.B.K., Craggs R.J., Shilton A.N., 2011. Recycling algae to improve species control and harvest efficiency from a high rate algal pond. Water Res. 45 (20), 6637-6649.

(19) Posadas, 2016. Innovative algal-bacterial processes for wastewater treatment: a further step towards full scale implementation: http://uvadoc.uva.es/handle/10324/18777.

(20) Posadas E., García-Encina P. A., Soltau A., Domínguez A., Díaz I., Muñoz R., 2013. Carbon and nutrient removal from centrates and domestic wastewater using algal-bacterial biofilm bioreactors. Bioresour. Technol. 139, 50-58.

(21) Posadas E., Morales M. M., Gómez C., Acién F. G., Muñoz R., 2015b. Influence of pH and CO_2 source on the performance of microalgae-based secondary domestic wastewater treatment in outdoors pilot raceways. Chem. Eng. J. 265, 239-248.

(22) Posadas E., Muñoz A., García-González M.-C., Muñoz R., García-Encina P. A., 2015c. A case study of a pilot high rate algal pond for the treatment of fish farm and domestic wastewaters, J. Chem. Technol. Biotechnol. 90 (6), 1094-1101.

(23) Posadas E., Serejo M., Blanco S., Pérez R., García-Encina P.A., Muñoz R., 2015a. Minimization of biomethane oxygen concentration during biogas upgrading inalgal–bacterial photobioreactors. Algal Res. 12, 221-229.

(24) Posadas E., Szpak D., Lombó F., Domínguez A., Díaz I., Blanco S., García-Encina P., Muñoz R., 2016. Feasibility study of biogas upgrading coupled with nutrient removal from anaerobic effluents using microalgae-based processes. J. Appl. Phycol. 28 (4), 2147-2157.

(25) Ryckebosch E., Drouillon M., Vervaeren H., 2011.Techniques for transformation of biogas to biomethane. Biomass. Bioenerg. 35 (5), 1633-1645.

(26) Sander R., 1999. Compilation of Henry's Law Constants for Inorganic and Organic Species of Potential importance in Environmental Chemistry (Last access: 30.11.2016): http://www.mpchmainz.mpg.de/sander/res/henry.html

(27) Serejo M., Posadas E., Boncz M., Blanco S., Garcia-Encina PA., Muñoz R., 2015. Influence of biogas flow rate on biomass composition during the optimization of biogas upgrading in microalgal-bacterial processes. Environ. Sci. Technol. 49 (5), 3228-3236.

(28) Sournia A., Phytoplanton Manual. Museum National d' Historie Naturelle, París, United Nations Educational, Scientific and Cultural Organization (Unesco), 1978.

(29) Toledo-Cervantes A., Madrid-Chirinos C., Cantera S., Lebrero R., Muñoz R., 2017. Influence of the gas-liquid flow configuration in the absorption column on photosynthetic biogas upgrading in algal-bacterial photobioreactors. Bioresour. Technol., 225, 336-342.

(30) Toledo-Cervantes A., Serejo M., Blanco S., Pérez R., Lebrero R., Muñoz R., 2016. Photosynthetic biogas upgrading to bio-methane: Boosting nutrient recovery via biomass productivity control. Algal Res., 17, 46-52.

(31) Tippayawong N., Thanompongchart P., 2010: Biogas quality upgrade by simultaneous removal of CO_2 and H_2S in a packed column reactor. Energy 35 (12), 4531-4535.

(32) Valigore J. M., Gostomski P. A. , Wareham D. G. , O'Sullivan A. D., 2012. Effects of hydraulic and solids retention times on productivity and settleability of microbial (microalgal-bacterial) biomass grown on primary treated wastewater as a biofuel feedstock. Water Res. 46, 2957-2964.

(33) Yan C., Muñoz R., Zhu L., Wang Y. (2016). The effects of various LED (light emittion diode) lighting strategies on simultaneous biogas upgrading and biogas slurry nutrient reduction by using of microalgae Chlorella sp. Energy 106, 554-561.

FIGURE CAPTIONS

Figure 1. Schematic diagram of the outdoors experimental set-up used for the continuous upgrading of biogas.

Figure 2. Time course of the concentration of (a) CH_4 (■), (b) CO_2 (♦) and H_2S (▲), and (c) O_2 (●) and N_2 (○) in the upgraded biogas. The removal efficiencies of CO_2 (◊) and H_2S (Δ) are also displayed in figure 2b.

Figure 3. Time course of the concentration of (a) CH_4, (b) CO_2, (c) O_2 and (d) N_2 in the upgraded biogas during the one-day cycle evaluated in stages I (♦), II (■) and III (▲).

Figure 4. Time course of the concentration of (a) CH_4, (b) CO_2, (c) O_2 and (d) N_2 in the upgraded biogas at L / G ratios of 0.5 (♦), 1 (□), 2 (▲) and 5 (○).

Figure 5. Time course of the influent (♦) and effluent (◊) concentrations of (a) TOC, (b) IC, (c) TN, (d) N-NH_4^+, (e) N-NO_2^-, (f) N-NO_3^-, (g) P-PO_4^{3-} and (h) SO_4^{2-} throughout the three operational stages.

Figure 6. Time course of the structure of microalgae population in the HRAP: (■) *Chlorella* sp., (▨) *Pseudanabaena* sp. and (□) *Chloroidium saccharophilum*.

Figure 1. Schematic diagram of the outdoors experimental set-up used for the continuous upgrading of biogas.

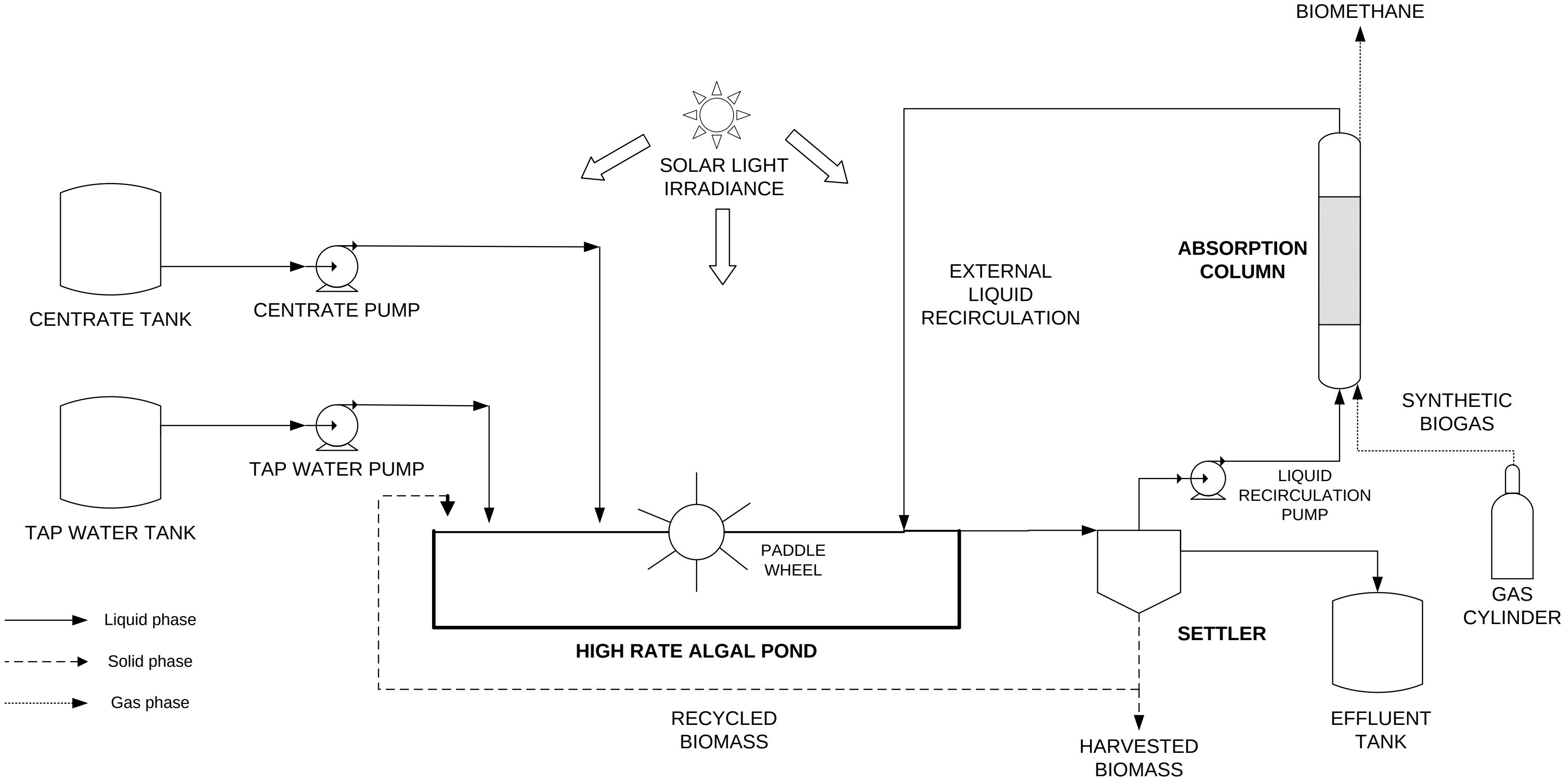

Figure 2. Time course of the concentration of (a) CH_4 (■), (b) CO_2 (♦) and H_2S (▲), and (c) O_2 (●) and N_2 (○) in the upgraded biogas. The removal efficiencies of CO_2 (◊) and H_2S (Δ) are also displayed in figure 2b.

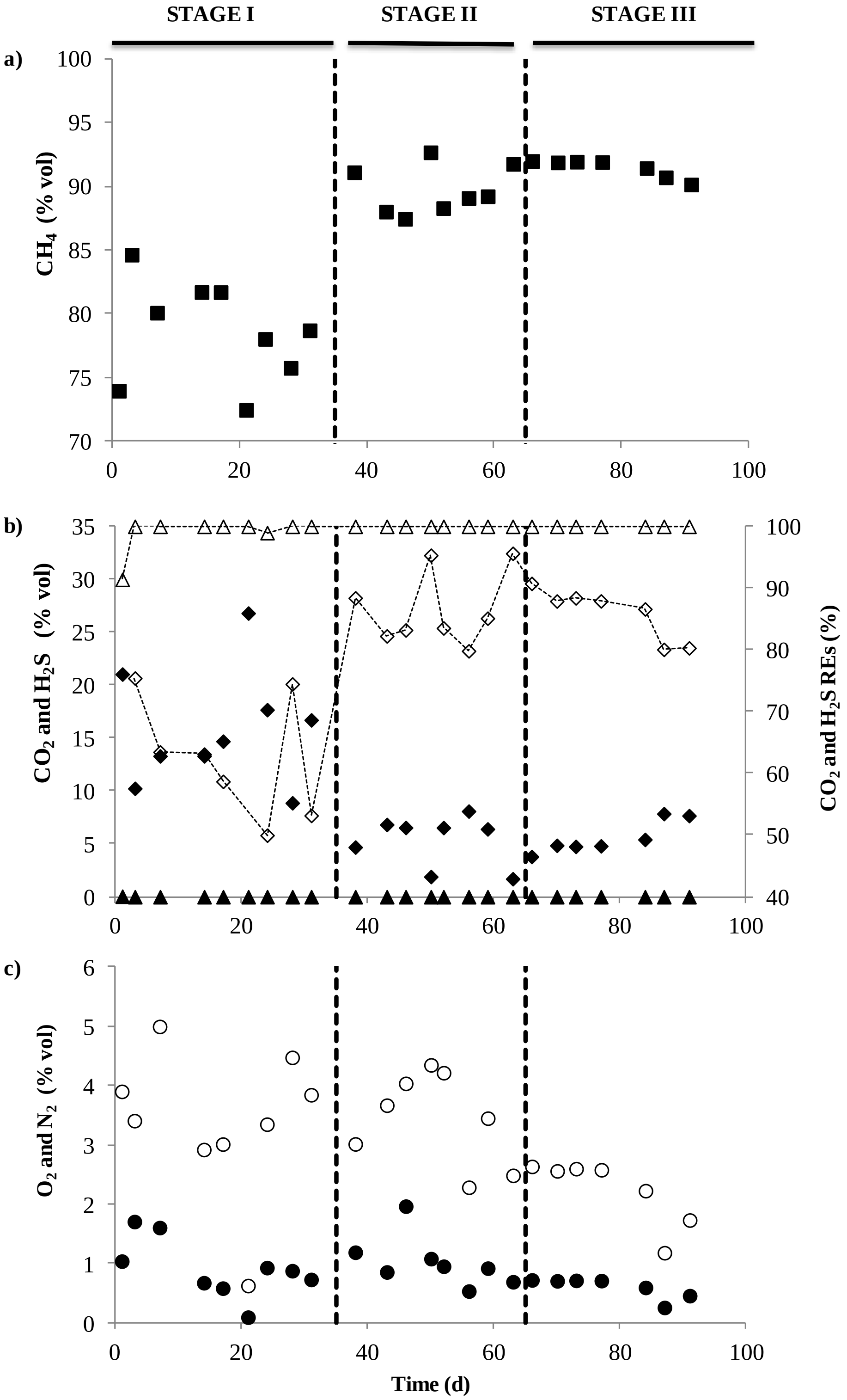

Figure 3. Time course of the concentration of (a) CH_4, (b) CO_2, (c) O_2 and (d) N_2 in the upgraded biogas during the diurnal cycle evaluated in stages I (♦), II (■) and III (▲).

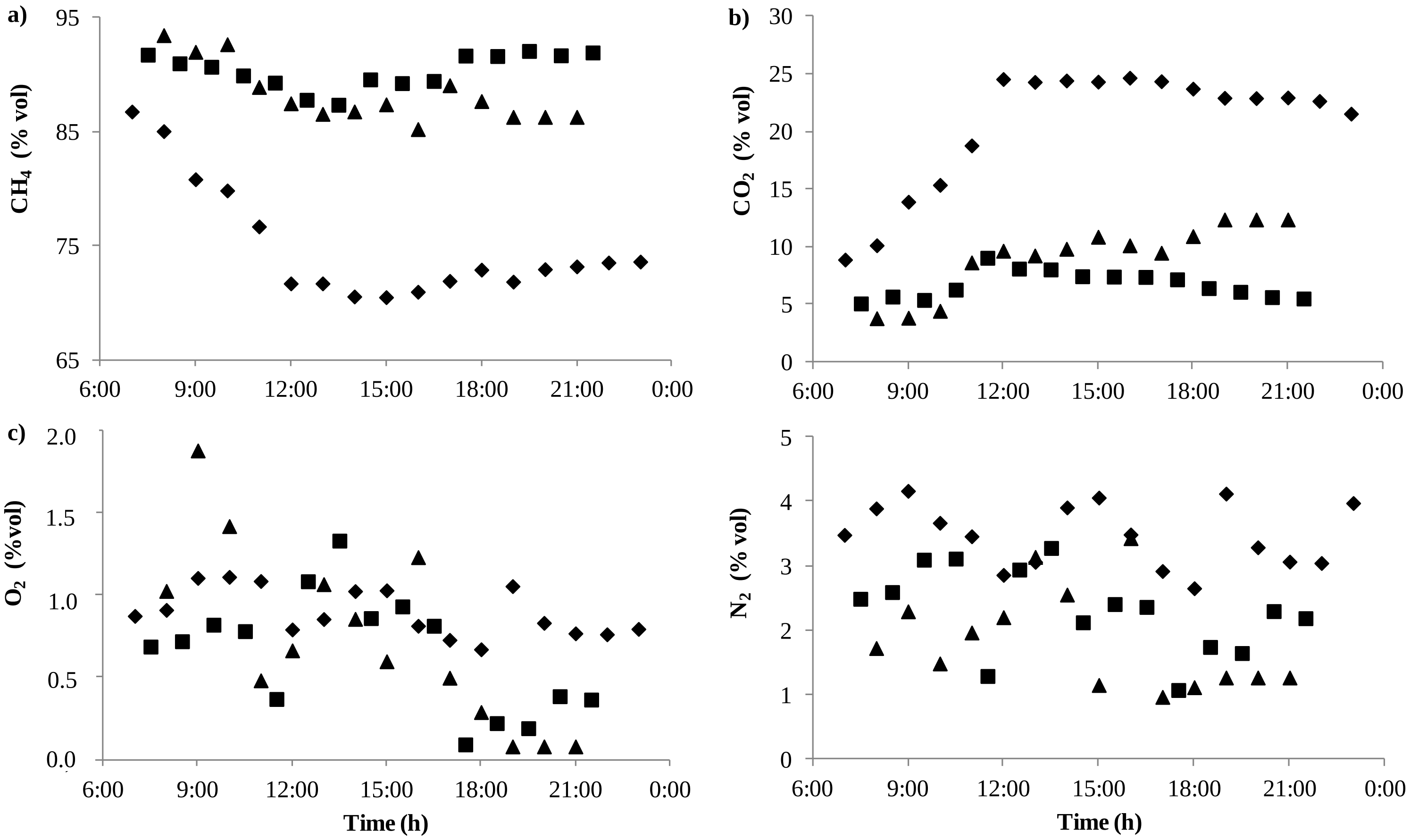

Figure 4. Time course of the concentration of (a) CH_4, (b) CO_2, (c) O_2 and (d) N_2 in the upgraded biogas at L / G ratios of 0.5 (♦), 1 (□), 2 (▲) and 5 (○).

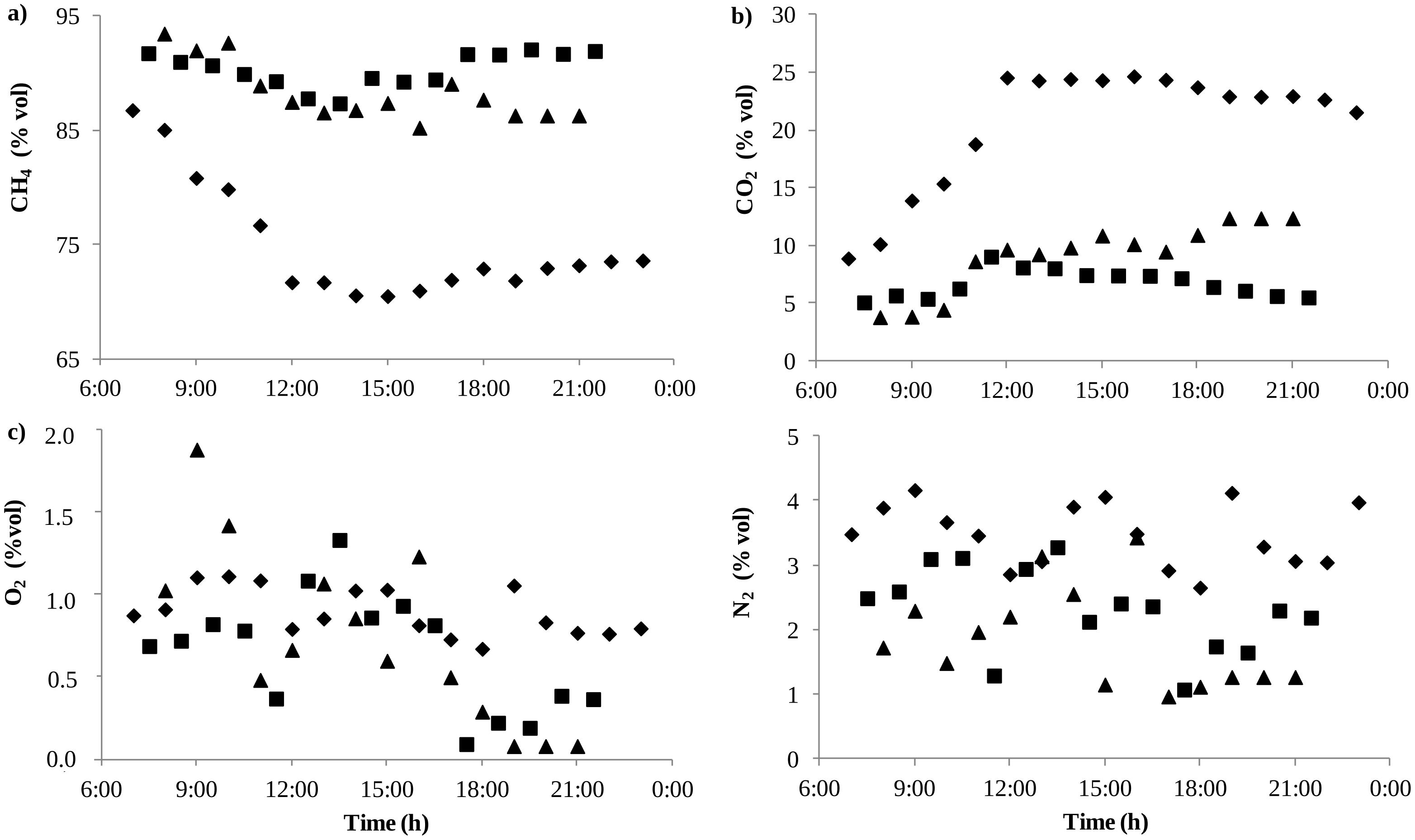

Figure 5. Time course of the influent (♦) and effluent (◊) concentrations of (a) TOC, (b) IC, (c) TN, (d) N-NH_4^+, (e) N-NO_2^-, (f) N-NO_3^-, (g) P-PO_4^{3-} and (h) SO_4^{2-} throughout the three operational stages

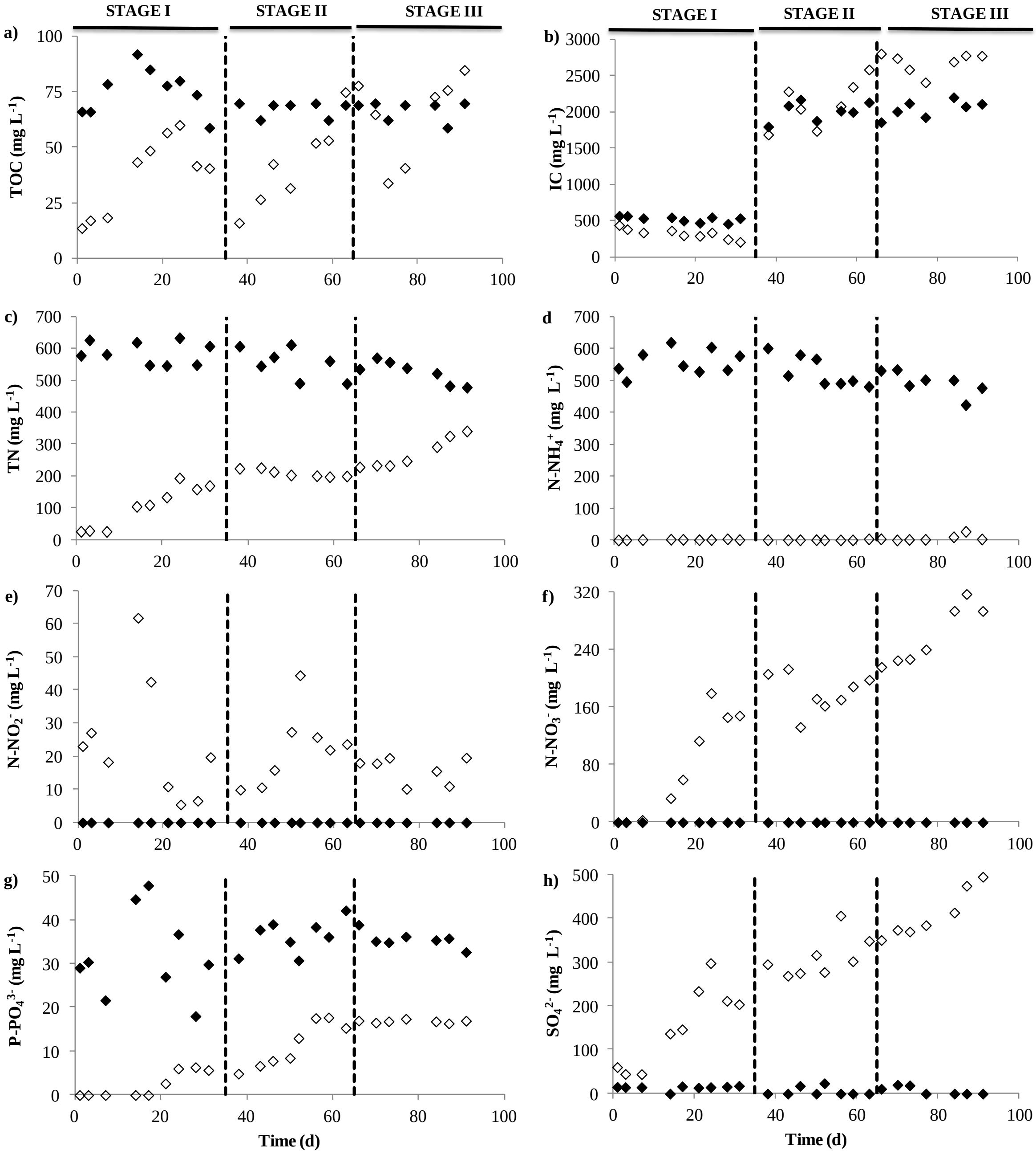

Figure 6. Time course of the structure of microalgae population in the HRAP: (■) *Chlorella* sp., (▨) *Pseudanabaena* sp. and (□) *Chloroidium saccharophilum*.

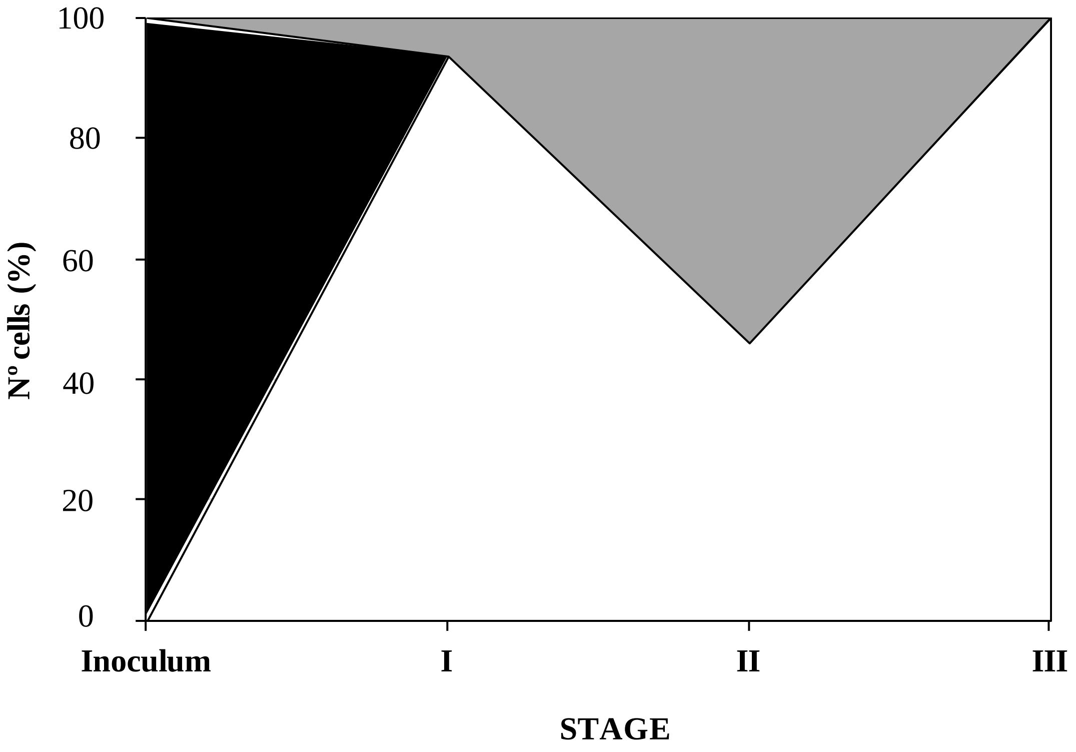

Table 1. Environmental and operational parameters during the three operational stages.

	STAGE		
PARAMETER	**I**	**II**	**III**
Date	05/07 - 08/08	09/08 – 06/09	07/09 – 04/10
Average temperature (ºC)	23.8 ± 6.7	23.5 ± 6.4	20.0 ± 6.7
Average PAR (µmol m^{-2} s^{-1})	1427 ± 65	1258 ± 140	946 ± 174
Number of sun hours (h)	12 ± 1	11 ± 1	9 ± 1
IC$_{influent}$ (mg L^{-1})	522 ± 40	2009 ± 135	2040 ± 120
Effluent from the settler (L d^{-1})	0.6	0.8	No effluent

Table 2. Steady state removal efficiencies of total organic carbon, total inorganic carbon, total nitrogen, ammonium and phosphorus during the three operational stages.

STAGE	**Removal efficiencies (%)**				
	TOC	**TIC**	**TN**	**N-NH_4+**	**P-PO_4^{3-}**
I	74±7	95±1	86±4	100±0	92±2
II	57±6	72±8	87±4	100±0	84±5
III	59±7	75±7	80±8	99±1	85±5

Table

Table 3. Carbon and nutrient recovery via biomass assimilation estimated from the carbon and nutrients removal, and the biomass elemental composition of the harvested biomass during stages I, II and III.

STAGE	**Carbon and nutrient recovery as biomass (%)**				**Biomass elemental composition (%)**			
	C	**N**	**P**	**S**	**C**	**N**	**P**	**S**
I	97±1	65±3	100±0	26±5	41.1	6.7	1.1	0.4
II	65±6	54±18	91±9	17±3	35.8	5.7	0.7	0.2
III	66±8	76±19	99±1	16±3	37.8	6.5	0.8	0.2